https://doi.org/10.61092/iaea.g3w9-n11v

INDC(NDS)-0738
Distr. G+NM+PH

IAEA
International Atomic Energy Agency

INDC International Nuclear Data Committee

ATLAS OF AVERAGE RESONANCE CAPTURE DATA

(STARTER FILE)

Prepared by

J. Kopecky
JUKO Research
Kalmanstraat 4, 1817 HX Alkmaar
The Netherlands

August 2017

IAEA Nuclear Data Section
Vienna International Centre, P.O. Box 100, 1400 Vienna, Austria

Selected INDC documents may be downloaded in electronic form from
http://www-nds.iaea.org/publications
or sent as an e-mail attachment.
Requests for hardcopy or e-mail transmittal should be directed to
NDS.Contact-Point@iaea.org
or to:
Nuclear Data Section
International Atomic Energy Agency
Vienna International Centre
PO Box 100
1400 Vienna
Austria

Printed by the IAEA in Austria

August 2017

INDC(NDS)-0738
Distr. G+NM+PH

ATLAS OF AVERAGE RESONANCE CAPTURE DATA

(STARTER FILE)

Prepared by

J. Kopecky
JUKO Research
Kalmanstraat 4, 1817 HX Alkmaar
The Netherlands

ABSTRACT

A resonance capture measurement is a direct method of determining experimentally the partial radiative width in a single-channel reaction mode and then converting it into the gamma-ray strength function. The capture is measured either on discrete resonances (using TOF spectrometry) or over a large number of resonances simultaneously (using filtered neutron beam). In this report, the *Average Resonance Capture* (ARC) data, measured at different filter beam facilities, are revisited and re-analysed. This includes all measurements performed in the period from 1970 to 1990, some of which are only partially exploited. The majority of these measurements were devoted to studying the spectroscopy of low-lying final states and only a very limited number of them addressed the *Photon Strength Function* (PSF) properties. The main aim of this work is to establish a complete data base of ARC measurements. The final Atlas file will include the selection of the best data converted in PSF for verification of different strength-function models.

August 2017

Contents

1. Introduction

Photon strength functions (PSF) describe the average response of the nucleus to an electromagnetic probe, and are thus a fundamental quantity of interest for modelling of nuclear reactions, and more particularly radiative capture. They are intimately connected to primary capture intensities which are, however, subject to Porter-Thomas fluctuations.

The ARC technique was developed to overcome the Porter-Thomas fluctuations of the primary intensities from thermal or isolated resonance capture data. It was realized that by simultaneous averaging over many resonances, the Porter-Thomas fluctuations could be reduced and the primary transitions to the final states of given J^{π} would have approximately the same intensity and could represent the distribution of the partial radiative width.

Three types of experiments are usually used, capture on discrete resonances using TOF spectrometry (DRC), the average resonance capture (ARC) with filtered beams and to a lesser extent thermal neutron-capture measurements (THC). The last method is preferable for nuclei where the thermal capture is dominated by a single strong s-wave resonance. The instrumental part and the basics of the average resonance capture method have been well documented in a number of previous surveys [1-6]. The main aspects of the statistical analysis are covered in references [7-11].

Three materials, ^{10}B, ^{45}Sc or ^{56}Fe, have been used for ARC experiments. The neutron beams are produced by transmission through filter materials which yield neutron beams with bell-shaped energy distributions and different full-width at half maximum (FWHM) at neutron energies of about 150 eV, 2 keV and 24 keV, respectively. The boron-filtered beam primarily removes the thermal component, while for Sc and Fe the thermal neutron capture cross section interference dips yield quasi mono-energetic beams of a few keV wide. Such facilities were established in four laboratories in the US: Argonne National Laboratory ANL [1], the National Bureau of Standards [2], the Idaho Nuclear Engineering Laboratory INEL [5] and Brookhaven National Laboratory BNL [6], during the period between 1970 and 1980. Outside the US, only three laboratories, two in USSR (IAEP/PPEI Obninsk [12] and Kiev [13]) and one in Germany (KfK Karlsruhe [14]), have ever published ARC data. The BNL facility turned out to be the best in all aspects, primarily due to high neutron fluence and superior processing tools, and therefore the majority of all adopted data originate from BNL.

The report is organized as follows. In Section 2 the ARC data from available measurements are presented. The conversion of the data into a strength function with a detailed description of the uncertainties is presented in Section 3. In Section 4 the re-evaluated final PSF are internally validated against the DRC data. Finally, in Section 4.3 the ARC E1 and M1 data are compared with recent calculations using an axially-symmetric-deformed HFB+QRPA model. Conclusions are presented in Section 5.

2. Data extraction

We have re-analysed all available ARC data measured at different beam facilities. The list of data sources used in this re-evaluation is given in the Appendix Table 1. It includes all measurements, which have been recovered from the period after 1970. Corresponding references are quoted. Some of the data, originating from the former collaboration between BNL (R.E. Chrien) and ECN (J. Kopecky), are referred here as *BNL/ECN database* and include both published and unpublished data. The objective of this effort was to form a complete starter file of ARC measurements to be used for determining PSF data; however, this was not completed at that time. All recovered data are listed, for those data not considered in this analysis the reason for exclusion is quoted in the comment column.

Both the ENSDF [http://www.nndc.bnl.gov/ensdf/] and EXFOR [http://www-nds.iaea.org/exfor/] databases were searched for relevant ARC publications and data. The search resulted in the selection of about 50 references with suitable data that could be retrieved and included in the compilation. Some of the data are included in a private database denoted as *BNL/ECN database*. However, the majority of publications focused on the spectroscopy of low-lying final states while only a few presented the measured data as PSF results [15-19]. The recommended set of data for the final f(L) database is shown in Table 2 of the Appendix.

The average differential strength function $<f_L>$, determined for a number of primary transitions with known multipolarity L, is defined as

$$<f_L\,(E_{\gamma i})> = << \Gamma_{\gamma i} >/ E^3_{\gamma i} > D_0^{-1}\ , \qquad (1)$$

where $\Gamma_{\gamma i}$ is the partial radiative width, $E_{\gamma i}$ is the transition energy and D_0 is the s-wave resonance spacing. While for DRC the partial radiative width $\Gamma_{\gamma i}$ is experimentally determined, for ARC measurements this quantity has to be derived from the normalization of the measured average gamma-ray intensity $<I_\gamma>$.

Note that for the DRC measurements, the parameters of the initial state are well defined by a single resonance (orbital momentum l and J^π) and the averaging over more resonances is carried out in the data processing. In contrast, in the ARC experiment the averaging is carried out in the experiment itself, due to the large number of resonances present in the filtered beam neutron window. However, as $<\Gamma_{\gamma i}>$ is not the measured observable, a normalization procedure has to be applied to extract it from the data (for further details see Sect. 3.3).

The results are usually given in reduced intensities either as $<I_\gamma/E_\gamma^3>$ (the phase factor) or as $<I_\gamma/E_\gamma^5>$ values (the assumed energy dependence of the Brink-Axel model) in arbitrary units. All retrieved measurements have been reanalysed and the resulting $<I_\gamma/E_\gamma^3>$ values form the starter database of ARC data (*AtlasIgE3*). The *AtlasIgE3* file includes all recovered data, even if the same reaction was studied by several authors. The main goal was to convert all the data (often presented also as I_γ only) into the common I_γ/E_γ^3 format and, furthermore, to reconfirm the multipolarity assignments of E1, M1 and E2 groups. For this purpose, for every target entry the corresponding final states with their Jπ assignmets, taken from the recent ENDSF file, are included and compared with the previous assignments. For some

transitions the corresponding final state was not quoted or was in conflict with the assignment, and for these cases the 24 keV data were also used as for confirmation. In particular, the kinematic shift between 2 and 24 keV data was employed and furthermore the standard 2/24 keV intensity ratio was used for parity assignment. An example of the input file is shown in Table 2 in the Appendix.

All errors quoted in the retrieved publications have been adopted as experimental statistical errors, without any modifications, in the *AtlasIgE3* database. They include the uncertainty of the gamma-ray spectrum analysis, namely the statistical accuracy and absolute intensity calibration. These errors are derived from the spectrum fitting and calibration treatment, and for moderately large and strong transitions, they are of the order of 10 - 20%. However, for transitions at lower gamma-ray energies with a high density of γ-lines or transitions with peak intensity close to the experimental sensitivity limit, these errors may be much larger.

3. PSF data processing

3.1. Data dispersion (final state population dependence)

The first reason for data dispersion is the dependence of averaged intensities on the spin of the final state. This is due to the different population of final state spin J_f groups ($J_t \pm 1/2$ and $J_t \pm 3/2$) from the initial s-wave capture state with $J_i = J_t \pm 1/2$ (see Fig. 1) and J_t the target spin. For data adopted from the BNL/ECN database, the dependence of averaged reduced intensities on the spin of the final state has been removed using the SPARC or RACA codes (Refs [7], [8]). Where such analysis is missing, an approximate factor based on the equation for the statistical factor

$$Q(J_iJ_f) = (J_i + ½) / 2(J_t + ½) \qquad (2)$$

has been used. As shown in Ref. [8], such an approximation does not significantly influence the results compared to the Monte-Carlo approach and the differences still remain within the statistical accuracy of the I_γ/E_γ^3 values.

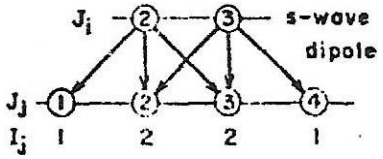

FIG. 1. *Schematic picture of double population of $J_i \pm 1/2$ final spin.*

The $Q(J_iJ_f)$ correction factors used for f(L) data files are shown in Table 1 for different spin configurations involved. The RACA calculated values are combined with a simplified approach, using the statistical factors for the generation of the capture states with spins J_i.

TABLE 1. THE CORRECTION FACTORS FOR THE (J_i -> J_f) POPULATION DEPENDENCE ON THE FINAL SPIN J_f.

Nucleus	$J_{t\pi}$	$Q(J_iJ_f)$ Stat. factor	$Q(J_iJ_f)$ RACA code
As-76	3/2-	2	
Zr-92	5/2+	2	
Mo-96	5/2+		2.02/1.8
Mo-98	5/2+	2	
Ru-102	5/2+		2.04/1.8
Pd-106	5/2+	2	
Cd-114	1/2+		1.62
Te-124	1/2+	1.33	
I-128	5/2+	2	
Ba-135	0+	1	1
Ba-136	3/2+	2	
Nd-146	7/2-	2	
Sm-155	0+	1	1
Gd-155	0+	1	1
Gd-156	3/2-	2	
Gd-157	0+	1	1
Gd-158	3/2-	2	
Gd-159	0+	1	1
Dy-162	5/2+		2.02/1.9
Dy-163	0+	1	1
Dy-164	5/2-		2.03/1.9
Dy-165	0+	1	1
Ho-166	7/2-	2	
Er-168	7/2+		2.32/1.7
Yb-172	1/2-		1.51
Yb-174	5/2-	2	
Lu-176	7/2+		2.02/1.9
Hf-178	7/2-	2	
W-184	1/2-	1.33	
W-185	0+	1	1
W-187	0+	1	1
Os-188	1/2-	1.33	
Os-189	0+	1	1
Os-191	0+	1	1
Os-193	0+	1	1
Ir-192	3/2+	2	
Ir-194	3/2+	2	
Pt-195	0+	1	1
Pt-196	1/2-	1.33	

Nucleus	$J_{t\pi}$	$Q(J_iJ_f)$ Stat. factor	$Q(J_iJ_f)$ RACA code
Pt-197	0+	1	1
Pt-199	0+	1	1
Au-198	3/2+	2	
Th-233	0+	1	1
U-236	7/2-	2	
U-239	0+	1	1
U-239	0+	1	1
Pu-240	1/2+	1.33	

3.2. Data dispersion from Porter-Thomas fluctuations

A major source of data dispersion are the Porter Thomas fluctuations. In an analysis of the BNL measurements, the Porter-Thomas uncertainty is estimated from the Monte-Carlo simulation code RACA [8]. This estimate is applied as an uncertainty band over data points for the same multipolarity and is not added to individual transitions as an additional error. Since the code RACA is not available anymore, we have searched for an alternative approach, which was employed before the code RACA was implemented in the ARC processing procedure.

Such a simple approach which can be treated as a useful approximation is the following: The relative variance is given by the factor $2/\upsilon$, where υ is the number of degrees of freedom. In the present situation υ is equal to the number of resonances present in the 2 keV window and can be estimated from the FWHM of the Sc filter. In the adopted data, the E1, M1 and sometimes E2 groups are clearly separated from each other due to the satisfactory experimental averaging and their multipolarity assignments are well known. The FWHM of the BNL Sc filtered beam facility has been determined to be 900 eV [6] and the number of resonances can be estimated using $\upsilon = 900/D_0$ (eV). This results in a dispersion $dPT = \sqrt{2/\upsilon}$. For a boron filter the FWHM is estimated at about 1000 eV [11].

The beam profile has the maximum neutron flux at its centre and reduced flux at the beam boundaries, leading to a reduction of the effective number of degrees of freedom, and the number of resonances. This can be compensated by using a smaller effective FWHM value of 600 eV. Furthermore, the presence of p-wave resonances may influence the dispersion (see following sections). Nevertheless, despite all these effects, this simple approximation gives sufficient information to evaluate the dispersion of the data due to the Porter-Thomas fluctuations within the E1, M1 and E2 experimental data groups and extract useful numbers. The derived PT dispersion factors for all studied nuclides are shown in Table 2.

TABLE 2. THE ESTIMATED PT DISPERSION FOR ALL NUCLIDES. FOR D_0 DATA FROM RIPL-3 HAVE BEEN USED [20].

Nucleus	D_0	$1+dPT = \sqrt{2}/\upsilon$	
	[eV]	FWHM n-beam 900keV	600keV
As-76	93	1.44	1.56
Zr-92	536	2.10	2.34
Mo-96	81.4	1.43	1.52
Mo-98	46.5	1.32	1.39
Ru-102	18.5	1.20	1.25
Pd-106	10.9	1.16	1.19
Cd-114	24.8	1.23	1.29
Te-124	25.1	1.24	1.29
I-128	9.7	1.15	1.18
Ba-135	360	1.89	2.09
Ba-136	40	1.29	1.36
Nd-146	17.8	1.13	1.19
Sm-155	114	1.50	1.62
Eu-154	1.14	1.05	1.12
Gd-155	13.8	1.17	1.21
Gd-156	1.8	1.06	1.08
Gd-157	30.5	1.26	1.32
Gd-158	87	1.44	1.54
Gd-159	82	1.43	1.52
Dy-162	2.14	1.07	1.09
Dy-163	62.9	1.37	1.46
Dy-164	7.28	1.13	1.16
Dy-165	144	1.57	1.69
Ho-166	4.20	1.07	1.09
Er-168	4	1.10	1.12
Tm-170	7.28	1.13	1.21
Yb-172	6.08	1.12	1.14
Yb-174	8.06	1.13	1.16
Lu-176	3.45	1.09	1.11
Hf-178	2.4	1.07	1.09
Ta-182	4.17	1.10	1.17
W-184	12	1.16	1.20
W-185	81	1.42	1.52

Nucleus	D_0	$1+dPT = \sqrt{2}/\upsilon$	
	[eV]	FWHM n-beam 900keV	600keV
W-187	93	1.46	1.56
Os-188	4.56	1.10	1.12
Os-189	40	1.29	1.36
Os-191	70	1.39	1.48
Os-193	115	1.51	1.62
Ir-192	1.68	1.06	1.07
Ir-194	3.98	1.09	1.11
Pt-195	82.6	1.43	1.53
Pt-196	19.2	1.21	1.25
Pt-197	214	1.69	1.84
Pt-199	340	1.87	2.07
Au-198	15.7	1.19	1.23
Th-233	15.8	1.19	1.23
U-236	0.49	1.03	1.05
U-239	16.4	1.19	1.23
Pu-240	2.07	1.07	1.08

For illustration, the PT dispersion band for E1 and M1 transitions of ^{197}Au(n,γ) reaction are shown in Fig. 2. The calculated trend lines were applied to guide the eye and are broadened by the estimated factor (1 + dPT) = 1.19. It seems that the number of outliers, considering the statistical errors, is reasonably small. The resonances from the tails of the bell shape neutron spectrum are weak and contribute less to the averaging.

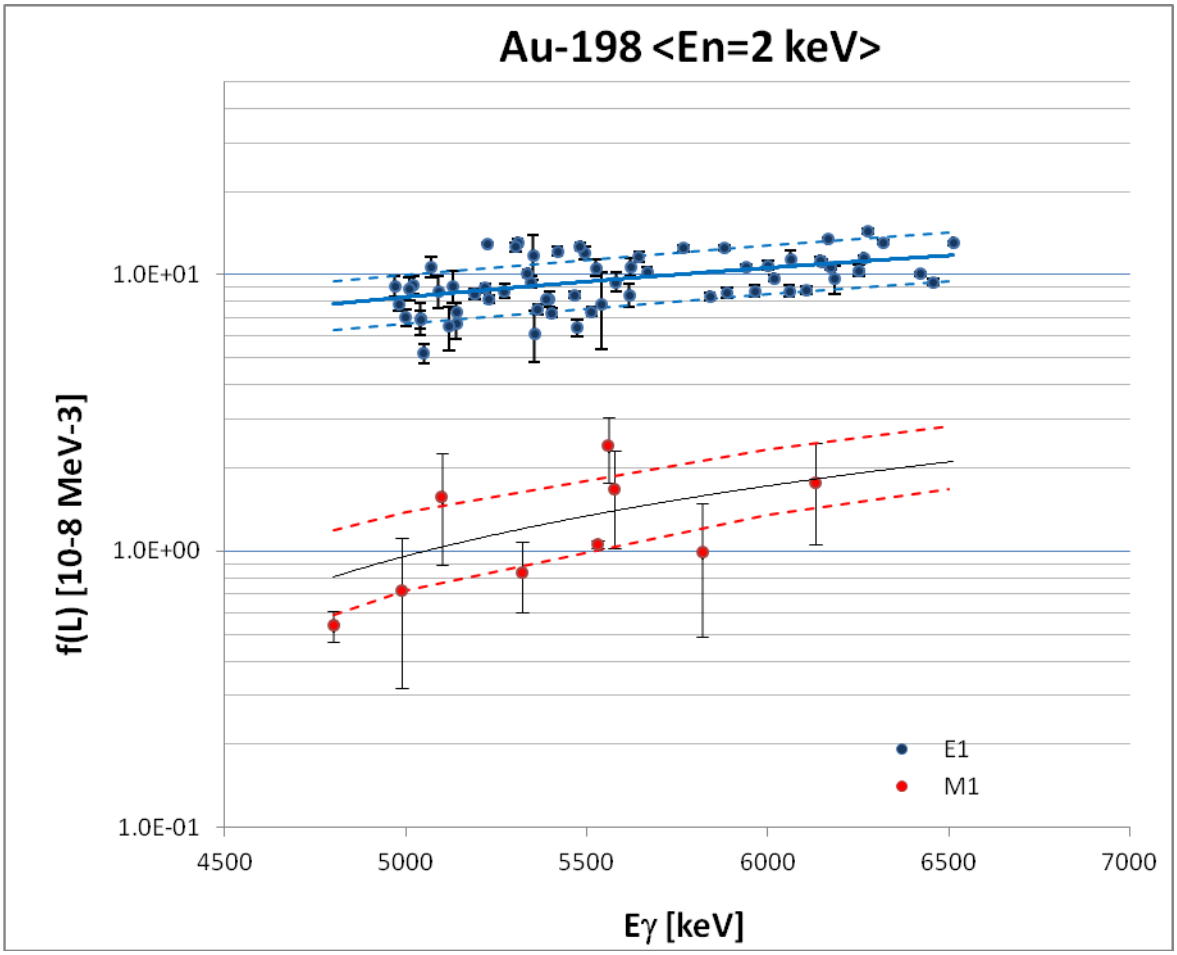

FIG. 2. *The PT dispersion estimated from the* $\sqrt{2/\upsilon}$ *approximation for* ^{198}*Au. The 2 keV data are taken from Atlasf(L) file. The trend fit curves (full and the dashed) describe the PT dispersion boundary around the arbitrary mean value.*

To illustrate this effect the dPT is also shown for a smaller window in order to accommodate this effect by smaller effective FWHM. However, the comparison of the $\sqrt{2/\upsilon}$ approximation with the Monte Carlo calculation (Refs [9], [21]) indicates that the influence is not significant in the case of data with small statistical errors.

3.3. Conversion to the absolute PSF scale

After the data are corrected for double population (see Fig. 1), the adopted $\langle I_\gamma/E_\gamma^3 \rangle$ values are converted into the γ-ray strength function scale of 10^{-8}MeV^{-3}. Because the initial state in the filtered beam experiments is a mixture of many initial states (resonances) and cannot be uniquely defined, some external information from other measurements is needed. In fact, the only way to generate absolute PSF from ARC filtered beam experiments is by normalizing the ARC data to the Γ_γ obtained from DRC. The DRC is the same physical process as ARC at similar neutron energy, however the resonances are resolved with well-defined orbital momentum and parity parameters, and therefore have known Γ_γ.

The calibration of the reduced intensities is performed by comparing with DRC data using equations

$$<f(I_\gamma/E^3)_{ARC}>/<f(E1)_{DRC}> = C \qquad (3)$$

and

$$f(E1)_{ARC} = C \times (I_\gamma/E^3)_{ARC} \qquad (4)$$

The E1 transitions are primarily used because of their superior statistical accuracy and their purity (the negligible effect of p-wave contribution). The calibration against DRC f(M1) values has not been used for two reasons: firstly the statistical accuracy is inferior to E1 data and, secondly, the M1 radiation from the capture of 2 keV neutron beam is slightly contaminated by E1 radiation from the p-wave capture (see below).

The normalization constant C may be derived in two ways. When DRC measurements are available, the information can be taken using the mean value of $f(E1)_{DRC}$, averaged over transitions present in the energy range used (usually of about 1 MeV broad), as documented in Ref. [22]. The advantage of this procedure is that the same transitions measured in both DRC and ARC experiments are used. The DRC then gives the absolute transition strength.

If the DRC measurement is not available, use is made of the f(E1) systematics

$$<f(E1)> = 0.0021 \cdot A^{1.69\pm0.17}\ [10^{-8}\ MeV^{-3}], \qquad (5)$$

which is based on a fit to measured DRC data [22]. The fitted average strength is given as a function of the atomic mass A at E_γ energies around 6.2 ± 0.5 MeV and is shown in Fig. 3. The fact that the fit is for a given E_γ window may be an additional source of uncertainty for targets for which the dominant E1 transitions are not in the vicinity of 6.2 MeV. In such a case, the systematic value has to be adjusted assuming an additional E^2 dependence from the Brink-Axel model.

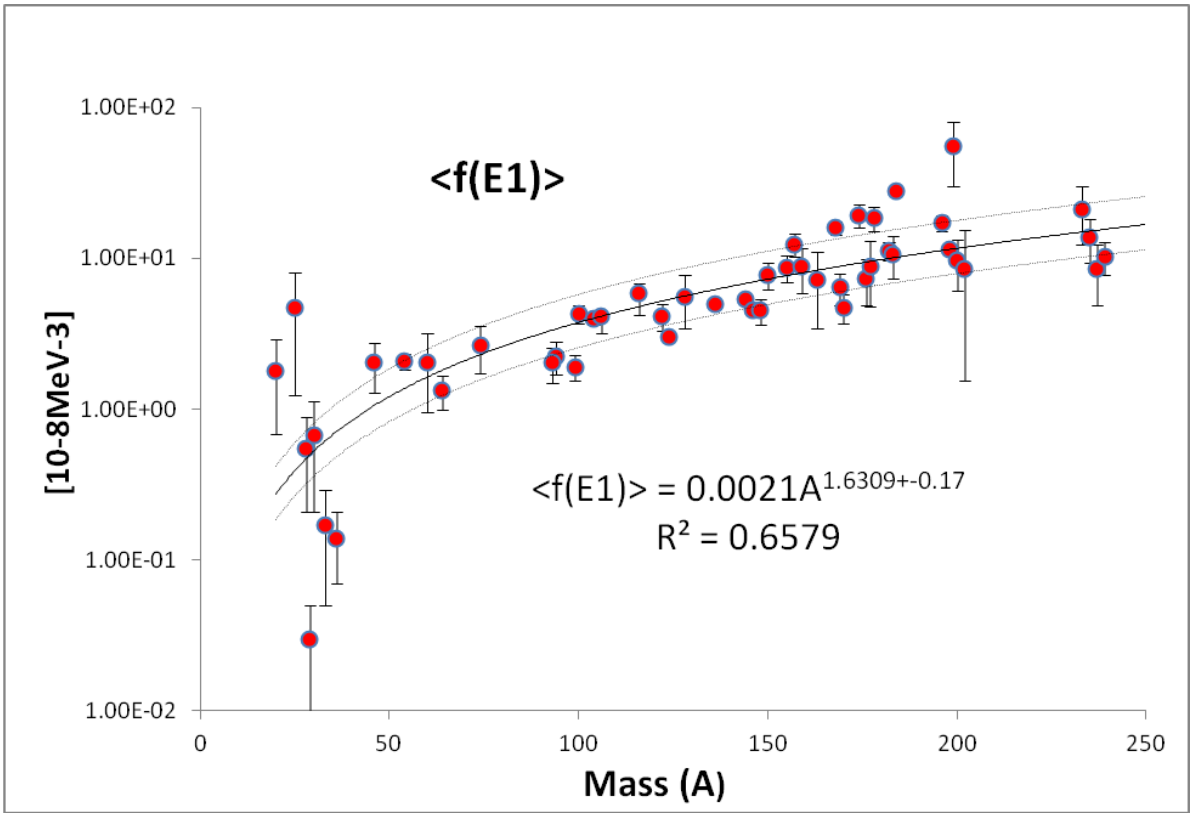

FIG. 3. *Plot of <f(E1)>$_{DRC}$ values. The full curve represents the LSQ fit to recent data with the R^2 value. The uncertainty band of f·A and A/f represents the 99% confidence limit. The mean energy <E_γ> of transition groups was 6.2 MeV.*

After completion of this re-analysis and re-processing, a recommended value was proposed for the PSF file (*Atlasf(L)*). For targets with more measurements, the quality and the completeness of data were used as a criterion to propose the recommended final source. The preliminary release of *Atlasf(L)* in March 2017 was used in Ref. [19].

An example of such a conversion is shown in in the Appendix (Table 3) for the ^{75}As(n,γ) reaction. The E1 transitions taken into account in the normalization procedure, in this case they were normalized to the systematics equation, are labelled in red and the M1 transitions, used for E1/M1 ratio analysis, are in blue. Note the energy range has been chosen close to 6-7 MeV and covers both E1 and M1 transitions. The summary of the normalization factors is included in Table 3.

TABLE 3. LIST OF NUCLIDES WITH THE ARC CALIBRATION IN TO THE PSF DATA
(The underlined data were used for the calibration)

Nucleus	n-beam	$<E_\gamma>$ Calib. energy	<f(E1)> E1 Calib. DRC exp.	<f(E1)> E1 Calib. DRC SYS
		MeV	$10^{-8}MeV^{-3}$	
As-76	Sc	6.7		2.35
Zr-92	Sc	6.2	--	3.20 M1)
Mo-96	Sc	6.1		3.43
Mo-98	Sc	6.6		3.55
Ru-102	Sc	6.8		3.78
Pd-106	B	7.2	4.14	(4.03)
Cd-114	Sc	6.2		4.53
Te-124	Sc	7.1	--	1.44 M1)
I-128	Sc	6.6	(1.90)	5.47
Ba-135	Sc	5.1		5.96
Ba-136	Sc	6.6	5.0	(6.03)
Nd-146	B	6.4	4.5	(6.77)
Sm-155	Sc	5.4		7.46
Eu-154	Sc	7.9		7.38
Gd-155	Sc	5.9	9.2	(7.46)
Gd-156	B	7.4		7.53
Gd-157	Sc	5.9	12.4	(7.61)
Gd-158	B	6.4		7.69
Gd-159	Sc	5.4	8.81	(7.77)
Dy-162	Sc	6.8		8.01
Dy-163	Sc	5.7	7.26	
Dy-164	Sc	7.2	8.17	(8.09)
Dy-165	Sc	5.4		8.24
Ho-166	B	6.0		8.33
Er-168	B	6.4	15.9	(8.50)
Tm-170	Sc	6.1	(4.72)	8.66
Yb-172	Sc	6.8		8.83
Yb-174	B	6.6	19.4	(8.99)
Lu-176	Sc	5.9	7.4	(9.16)
Hf-178	Sc	6.8	18.5	(9.33)
W-184	B	6.8	28.1	(9.85)
W-185	Sc	5.4		9.93
W-187	Sc	4.6		10.11

Nucleus	n-beam	<E_γ> Calib. energy	<f(E1)> E1 Calib. DRC exp.	<f(E1)> E1 Calib. DRC SYS
		MeV	$10^{-8}MeV^{-3}$	
Ta-182	Sc	5.8	11.3	(9.67)
Os-188	Sc	6.3		10.20
Os-189	Sc	4.5		10.28
Os-191	Sc	5.4		10.46
Os-193	Sc	5.5		10.60
Ir-192	Sc	6.1		10.55
Ir-194	Sc	5.9		10.73
Pt-195	Sc	4.9		10.82
Pt-196	Sc	6.3	17.4	(10.91)
Pt-197	Sc	4.7		11.00
Pt-199	Sc	4.6		11.18
Au-198	Sc	6.0	11.4	(11.09)
Th-233	Sc	4.1	(20.3)	14.44
U-236	Sc	6.0		15.6
U-239	B	4.0	10.29	(15.04)
Pu-240	Sc	5.6	19.9	(15.15)

<E_γ> the mean energy of the energy interval of transitions used for the calibration
<f(E1)> PSF values derived from DRC or systematic, underlined values adopted
M1 No E1 transitions present, M1 systematic used instead

3.4. The <E_γ> dependence of the normalization

The mean energy of the energy regions (on average about 0.5 – 1 MeV wide), used for normalization of the I_γ/E_γ^3 input data, is shown in the first column of Table 5. They range between 3.6 and 7.2 MeV. In cases where the measured DRC data are used for normalization and the identical transitions are also chosen, no energy difference between DRC and ARC data occurs. However, the situation is different if the ARC data are normalized to the DRC systematics. The average reference energy of the <f(E1)> systematics equation is 6.2 ± 0.25 MeV while some of the used energy regions of the ARC data are significantly different. In such cases, for the renormalization to this energy a correction factor has to be applied. The additional energy dependence is generally assumed to be E_γ^2 as predicted by the Brink-Axel Giant Resonance model. The resulting <E_γ> listing is given in Table 4.

TABLE 4. THE E_γ DEPENDENCE CORRECTION FACTOR F = $\langle E_\gamma \rangle_{ARC}/\langle E_\gamma \rangle_{DRC}$ *(for data normalized to the* $\langle f(E1) \rangle_{DRC}$ *from DRC measurements or DRC systematics at 6.2 MeV. The third column gives the* F^2 *ratio for DRC measurements, while the fourth column gives the DRC systematics).*

Nucleus	$\langle E_\gamma \rangle_{ARC}$	<DRC> F^2	< SYS> F^2
		used	used
As-76	6.7		0.86
Zr-92	6.2		1 M1
Mo-96	6.1		1.03
Mo-98	6.6		0.88
Ru-102	6.8		0.83
Pd-106	7.2	0.96	
Cd-114	6.2		1
Te-124	7.1	1 M1	
I-128	6.6	1.03	
Ba-135	5.1		1.48
Ba-136	6.6	1	
Nd-146	6.4	1.09	
Sm-155	5.4		1.32
Eu-154	7.9		0.62
Gd-155	5.9	1.20	
Gd-156	7.4		0.7
Gd-157	5.9	0.96	
Gd-158	6.4		0.94
Gd-159	5.4	0.89	
Dy-162	6.8		0.83
Dy-163	5.7		
Dy-164	7.2		0.74
Dy-165	5.4		1.32
Ho-166	6.0		1.07
Er-168	6.4	1	
Tm-170	6.1		1.03
Yb-172	6.8		0.82
Yb-174	6.6	0.95	
Lu-176	5.9	0.98	
Hf-178	6.8	0.95	
W-184	6.8	0.94	
W-185	5.4		1.32
W-187	4.6		1.82

Nucleus	$<E_\gamma>_{ARC}$	<DRC> F^2	< SYS> F^2
		used	used
Ta-182	5.8		
Os-188	6.3		0.97
Os-189	4.5		1.90
Os-191	5.4		1.32
Os-193	5.5		1.27
Ir-192	6.1		1.03
Ir-194	5.9		1.10
Pt-195	4.9		1.60
Pt-196	6.3		0.97
Pt-197	4.7		1.74
Pt-199	4.6		1.82
Au-198	6.0	1	
Th-233	4.1		2.29
U-236	6.0		1.07
U-239	4.0	0.94	
Pu-240	5.6	0.92	

The following nuclides, which are normalized to the DRC systematics but have $<E_\gamma>$ outside the 5.7 – 6.7 MeV range, have been corrected using the factor $(<E_\gamma>_{ARC}/6.2)^2$: ^{135}Ba, ^{155}Sm, ^{154}Eu, ^{156}Gd, ^{164,166}Dy, ^{185,187}W, ^{195,197,199}Pt and ^{233}Th.

3.5. The p-wave contribution

The ARC experiments use neutron beam energies spreading from about 100 eV (B) through 2 keV (Sc) and up to 24 keV (Fe). The dominance of s-wave capture, close to thermal energies, decreases with increasing neutron energy, as p-wave resonances start to contribute to the capture process. This effect has been included in the code RACA which performs Monte-Carlo modelling of the partial cross sections and is discussed in Refs. [8] and [9]. In spectroscopic applications of the ARC method, the p-wave capture is primarily used for the determination of the parity of the final states. This is done by taking the ratio of intensities of the 24 keV data to the 2 keV data. The boron filtered beam with its low neutron mean energy of about 150 eV has a negligible p-wave component, except for nuclides from the 3p-giant resonance of the p-wave strength around A = 100. In the present database, only the ^{106}Pd file is influenced by this p-wave contribution.

However, for PSF applications, the p-wave capture both at 2 keV and mainly at 24 keV, complicates the determination of the absolute strength of M1 radiation, as it causes an increase of the s-wave M1 strength by a p-wave E1 admixture. In all BNL/ECN data the p-wave admixture at 2 keV was estimated from RACA calculations and the results are shown in Table 4. The size of this contribution

follows the distribution of 3p and 4p giant resonances of p-wave neutron strength function. In contrast, the increase of the E1 s-wave capture by M1 p-waves is negligible due to the weaker M1 strength. In all calculated cases, the M1 p-wave contribution to E1 transitions was smaller than ±5% (see Table 6).

TABLE 6. THE RESULTS OF RACA CALCULATIONS OF THE P-WAVE COMPONENT AT 2 KEV ARC EXPERIMENTS *(from private BNL/ECN collaboration logbook).*

Nuclide	$\langle f(M1)\rangle_{p\text{-waves}}$ in $\langle f(E1)\rangle_{s\text{-waves}}$	$\langle f(E1)\rangle_{p\text{-waves}}$ in $\langle f(M1)\rangle_{s\text{-waves}}$
Mo-96	0.09	0.66
Ru-102	0.04	0.33
Cd-114	0.04	0.24
Sm-155	0.04	0.21
Gd-157	0.01	0.15
Dy-162	0.01	0.13
Dy-164	0.02	0.18
Yb-172	0.01	0.09
Lu-176	0.01	0.15
Pt-195	0.02	0.31
Th-233	0.02	0.39
U-239	0.03	0.37

For the ARC data included in the BNL-ECN database, the E1 component present in the M1 radiation was estimated by RACA code calculations. For the remaining data, with no corrections, this effect is estimated using a theoretical prescription detailed in Refs. [7-11]. According to this prescription, the formula for the ratio of s- and p-wave capture (e.g. given by Eq. 7 in Ref. [9]) is a function of several ingredients, such as S_0, S_1, $\Gamma_{\gamma 0}$ and $\Gamma_{\gamma 1}$. Assuming that, $\Gamma_n << \Gamma_{\gamma,}$ Γ_γ is independent of the orbital momentum and $D_J = D_0/2J+1$, the average cross section at 2 keV [9] can be approximated as

$$\langle\sigma_{Jf}\rangle \sim \Sigma_{s\text{-wave}} \langle\Gamma_{\gamma f}(E1,M1)\rangle + S_1 f/S_0 \; \Sigma_{p\text{-wave}} \langle\Gamma_{\gamma f}(E1,M1)\rangle \qquad (6)$$

The factor $f = (ka)^2/(1+(ka)^{2)}$ is the penetrability of p-wave neutrons relative to s-wave neutrons.

The dominant factor in this equation is the S_1/S_0 ratio. In Fig. 4 we plot the calculated $(f(E1))_{p\text{-wave}}/(f(M1)_{s\text{-wave}})$ ratio against the S_1/S_0 ratio, and use this scatter plot to estimate the E1 (p-wave) component. We used the RACA calculated contributions for 11 nuclides from the BNL/ECN collaboration (no S_1/S_0 value for ^{195}Pt).

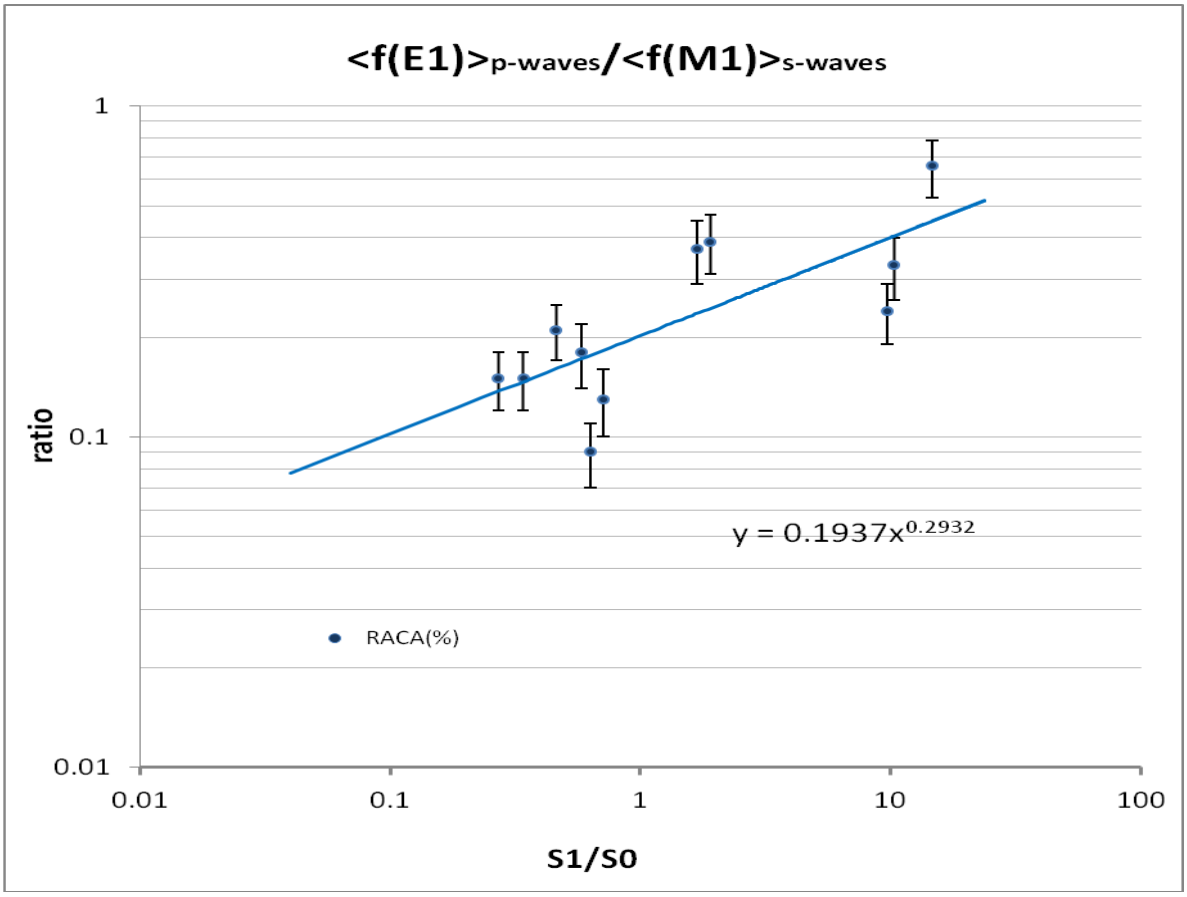

FIG. 4. *The calculated* $\langle f(E1)\rangle_{p\text{-}waves}/\langle f(M1)\rangle_{s\text{-}waves}$ *ratios as a function of* S_1/S_0*. The fitted trend line is used as a systematic estimate of the p-wave admixture.*

The scattered points are fitted by a trend function: $\langle f(E1)\rangle_{p\text{-}waves} / \langle f(M1)\rangle_{s\text{-}waves} = 0.19\cdot(S_1/S_0)^{0.29}$ which is then used to estimate this effect for all the nuclei in the ARC database. The resulting corrections applied to the M1 strength are included in Table 7.

TABLE 7. LIST OF NUCLIDES WITH THE P-WAVE CORRECTIONS.

Nucleus	n-beam	S_1/S_0	p-wave E1in M1 s-wave estimate	p-wave E1in M1 applied
As-76	Sc	0.96	0.19	0.19[3)]
Zr-92	Sc	18.1	0.45	0.45[3)]
Mo-96	Sc	14.66	0.43	0.66[1)]
Mo-98	Sc	23.79	0.49	0.49[3)]
Ru-102	Sc	10.34	0.38	0.33[1)]
Pd-106	B	10.27	0.36	0.33[4)]
Cd-114	Sc	9.68	0.37	0.24[1)]
Te-124	Sc	1.90 [a)]	0.23	0.23[3)]

Nucleus	n-beam	S_1/S_0	p-wave E1in M1 s-wave estimate	p-wave E1in M1 applied
I-128	Sc	2.57	0.26	0.26 [3]
Ba-135	Sc	1.77	0.23	0.23 [3]
Ba-136	Sc	1.3	0.21	0.21 [3]
Nd-146	B	1.10 [a]	0.20	0 [2]
Sm-155	Sc	0.68 [a]	0.17	0.21 [1]
Eu-154	Sc	2.20	0.24	0.24 [3]
Gd-155	Sc	0.75 [a]	0.18	0.18 [3]
Gd-156	B	1.68	0.23	0 [2]
Gd-157	Sc	0.34	0.14	0.15 [1]
Gd-158	B	1	0.19	0 [2]
Gd-159	Sc	0.81	0.18	0.18 [3]
Dy-162	Sc	0.71	0.17	0.13 [1]
Dy-163	Sc	0.63	0.17	0.17 [3]
Dy-164	Sc	0.58	0.16	0.18 [1]
Dy-165	Sc	0.7	0.17	0.17 [3]
Ho-166	B	0.54	0.25	0 [2]
Er-168	B	0.52	0.16	0 [2]
Tm-170	Sc	0.60 [a]	0.17	0.2 [3]
Yb-172	Sc	0.63	0.17	0.09 [1]
Yb-174	B	0.54	0.16	0.16 [3]
Lu-176	Sc	0.27	0.13	0.15 [1]
Hf-178	Sc	0.38	0.14	0.14 [3]
Ta-182	Sc	0.38	0.14	0.14 [3]
W-184	B	0.38	0.14	0 [2]
W-185	Sc	0.23	0.12	0.12 [3]
W-187	Sc	0.17	0.11	0.11 [3]
Ta-182	Sc	0.35	0.14	0.14 [3]
Os-188	Sc	0.2	0.12	0.12 [3]
Os-189	Sc	0.13	0.10	0.10 [3]
Os-191	Sc	[b]		0.2 [3]
Os-193	Sc	[b]		0.2 [3]
Ir-192	Sc	0.26 [a]	0.13	0.13 [3]
Ir-194	Sc	0.38 [a]	0.15	0.15 [3]
Pt-195	Sc	0.25 [a]	0.13	0.31 [1]
Pt-196	Sc	0.28 [a]	0.14	0.14 [3]

Nucleus	n-beam	S_1/S_0	p-wave E1in M1 s-wave estimate	p-wave E1in M1 applied
Pt-197	Sc	0.28 [a)]	0.14	0.14 [3)]
Pt-199	Sc	0.36 [a)]	0.15	0.15 [3)]
Au-198	Sc	0.84	0.18	0.18 [3)]
Th-233	Sc	1.79	0.23	0.39 [1)]
U-236	Sc	1.84	0.23	0.23 [3)]
U-239	B	1.68	0.22	0 [2)]
Pu-240	Sc	1.55	0.22	0.22 [3)]

S_1/S_0 S_0 and S_1 values taken from RIPL3
[a)] S_1 values estimated from Fig. 2.2 and DOM calculations in [BNL]
[b)] No S_0 value available

p-wave the estimated/calculated p-wave E1 contribution in M1 s-wave transitions at <En> = 2 KeV
[1)] RACA calculations (BNL-ECN data base[),]
[2)] boron estimate assumed with negligible p-wave contribution
[3)] empirical estimate in this work from $E1_p/M1_s = 0.19 \cdot S_1/S_0^{0.29}$
[4)] estimated from DRC data

All corrections from this section have been applied to the Atlasf(L) file and led to the final version of Atlasf(L)final (a file example is in Table 4 of the Appendix).

4. PSF internal validation

4.1. <f(M1)> comparison against DRC data

The M1 transitions were not used for f(L) normalization (except for two nuclides without E1 data), the reasons were discussed in Sect. 2.3. Therefore, the two sets of M1 data from DRC and ARC experiments are independent and can be used for comparison and validation. The results of the <f(M1)> comparison are shown in Fig. 5. The data can be compared directly in absolute units, because similar energy regions have been used in both experiments.

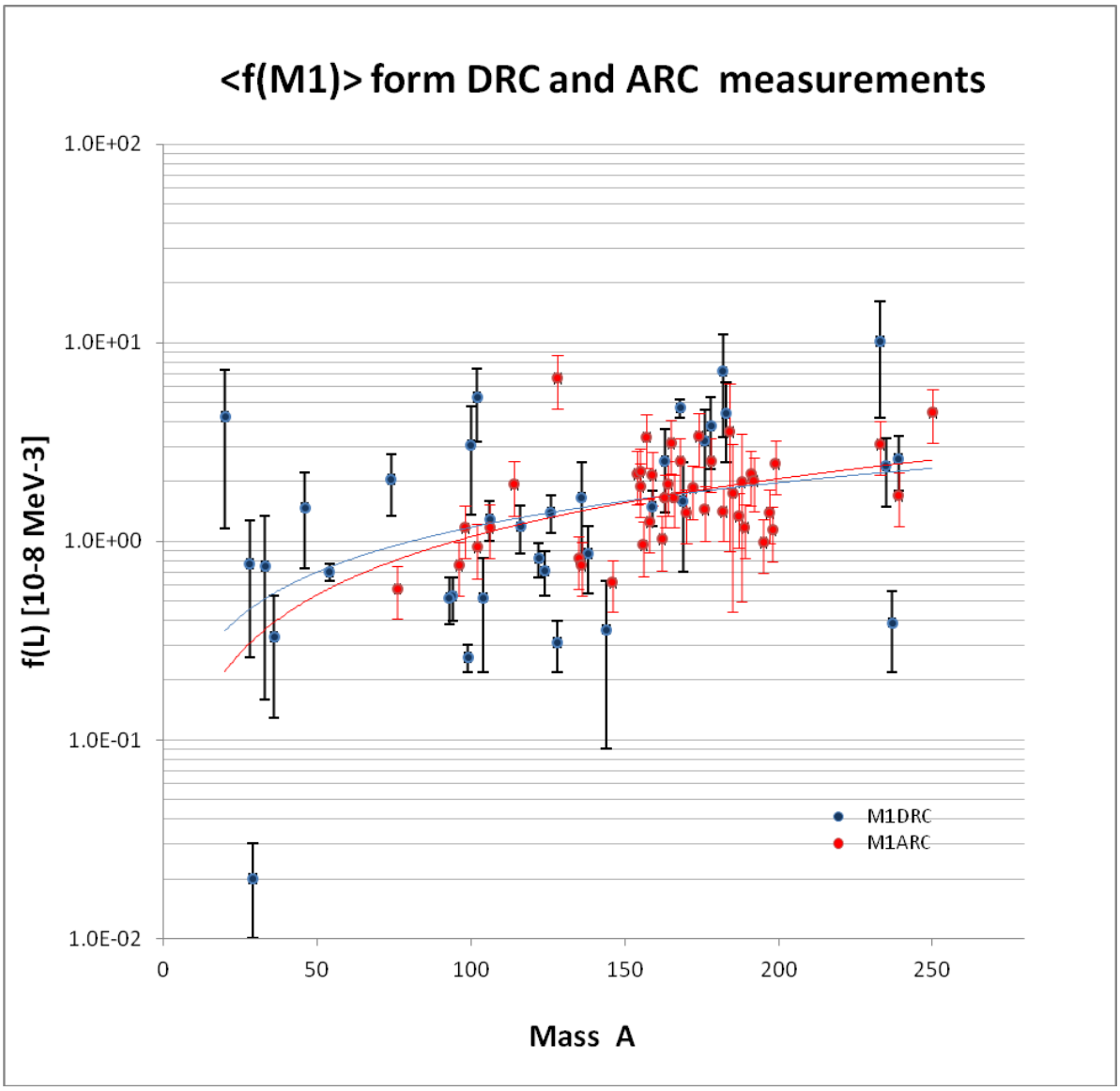

FIG. 5. *Comparison of <f(M1)> values from DRC measurements [18] and recent ARC data taken from the present Atlasf(L)[final] file.*

Both data sets are in very good agreement, which is also supported by two trend lines, which are close to each other. We may conclude that the adopted normalization procedure using exclusively E1 transitions gives good results for pure M1 strength.

4.2. The E1/M1 ratio in ARC and DRC (comparison)

While both the E1 and M1 strengths are affected by uncertainties as a result of the conversion from intensities I_γ/E_γ^3 into PSF format (as described in Sect. 3), the ratio of the E1 to M1 strength remains independent of the conversion procedure, provided the competing E1 contribution to M1 transitions for the p-wave capture is properly allowed for (see Sect. 3.5). We show in Fig. 6 the E1-to-M1 ratio as a function of the atomic mass A, both for the original ARC data at energies ranging between 3.6 and 7.2 MeV and for the data obtained after renormalizing the ARC data at the average reference energy of 6.2 ± 0.25 MeV. The energy regions of the E1 and M1 data used (on average about 1 MeV wide)

were identical in order to minimize the internal energy dependence between them. For the renormalization to the reference energy, an empirical factor, derived from the present ARC data, was applied. As can be seen in Fig. 6, the original E1/M1 ratio is broadly distributed between 1.5 and 7.8. However, note that this ratio is obtained at different energies and for nuclei that can be either spherical or deformed.

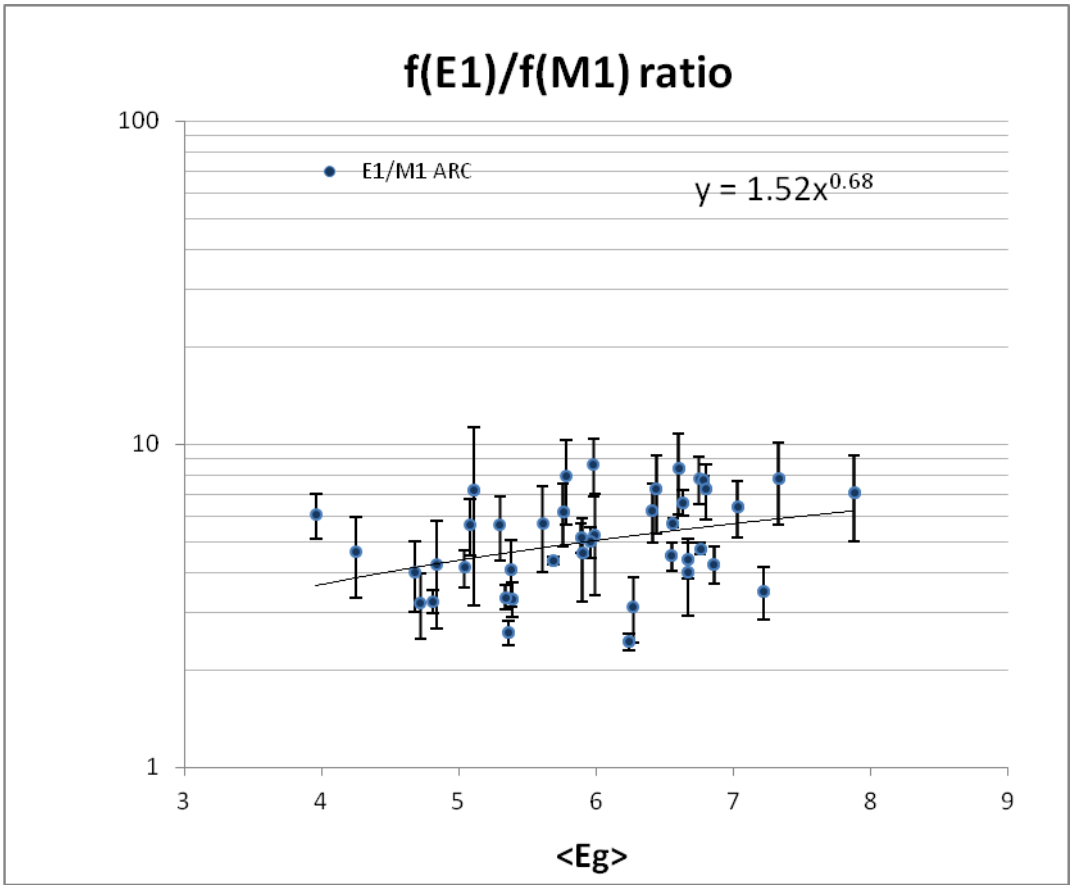

FIG. 6. *The energy dependence of <f(E1)>/<f(M1)> ratio as a function of the mean transition energy <E_γ>, taken from the present ARC data.*

It is therefore not recommended to use these data to extract systematics. Previous analyses of ARC data [22,23] led to systematics at the reference energy of 6.2 MeV that are described by the empirical function $f(E1)/f(M1) = 0.059 \cdot A^{0.87}$. This empirical function is the one recommended by the RIPL-3 library at the reference energy of 7 MeV [20]. With the additional data available now, we can further test and improve this systematics. As shown in Fig. 7, at the reference energy of 6.2 MeV, an average ratio $f(E1)/f(M1) = 0.35 \cdot A^{0.53}$ can explain the general trend. This agreement supports the compatibility of DRC and ARC measurements. However, as the observed dispersion around the systematics is rather large, these expressions should not be used for single events but rather for setting the general trend. This dispersion is partly due to the difference in the mean energy of <f(E1)> and <f(M1)> regions used for averaging and also to the variety of M1 excitation modes as a function of A.

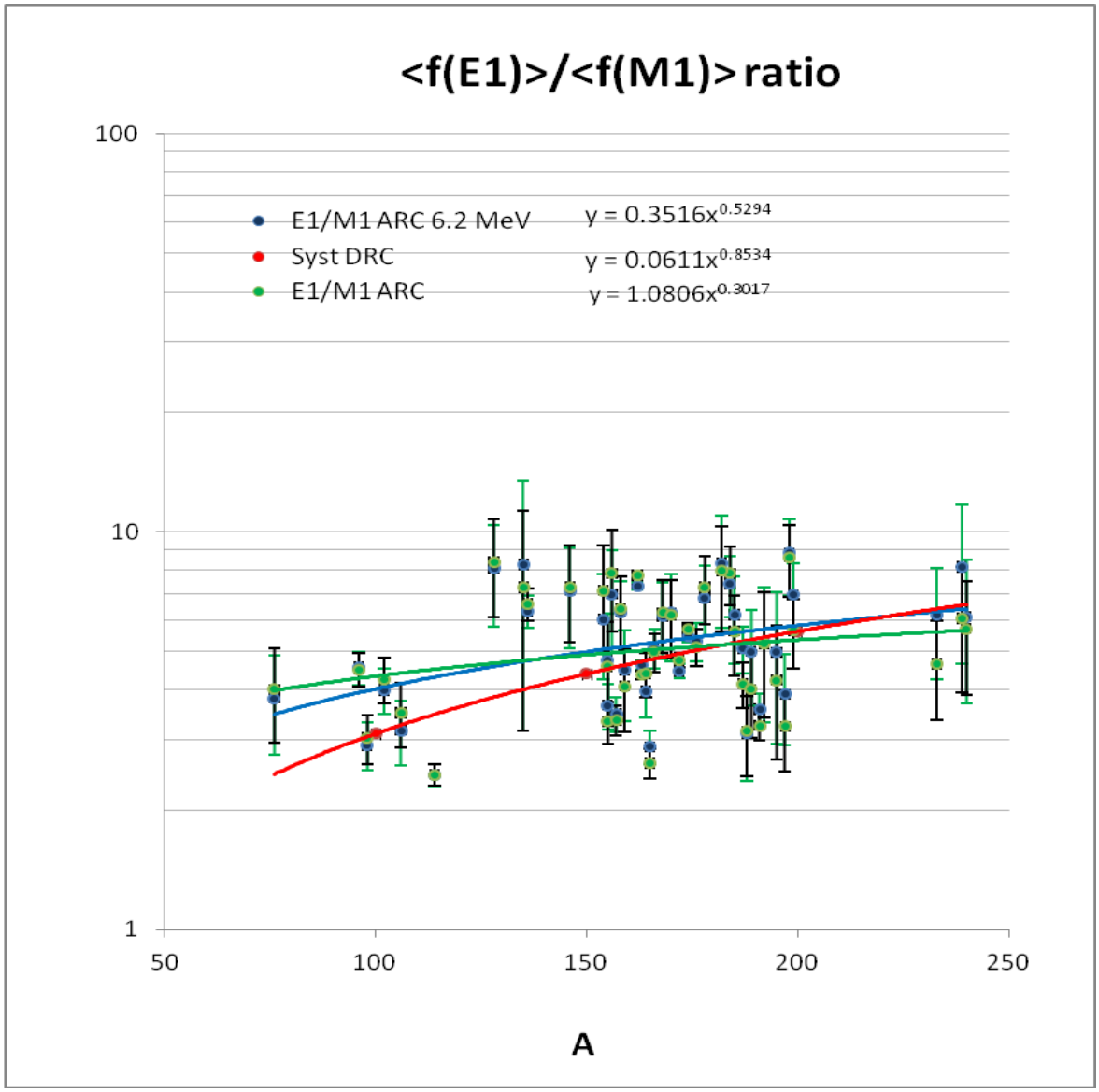

FIG. 7. *The E1 to M1 strengths ratio extracted from ARC data as a function of the atomic mass A. The green squares correspond to the ratio at the measured average energy and the blue squares renormalized at 6.2 MeV. The solid blue line is the newly proposed systematics of* $f(E1)/f(M1) = 0.35 \cdot A^{0.53}$ *at 6.2 MeV. The red line is the widely used RIPL-3 systematics* $f(E1)/f(M1) = 0.06 \cdot A^{0.85}$ *[20,23].*

4.3. The comparison with PSF models

The recently developed D1M+QRPA approach ([24,25]) has been chosen for the comparison of the final ARC data against model predictions. Most of the nuclei for which ARC data are available correspond to deformed nuclei, except for light nuclei such as ^{76}As, ^{92}Zr, ^{96,98}Mo, ^{146}Nd or ^{135,136}Ba, as seen by the M1 strength pattern from QRPA predictions (see an example in Fig. 8). All the results for E1 and M1 strength are shown in Figs. 9 and 10.

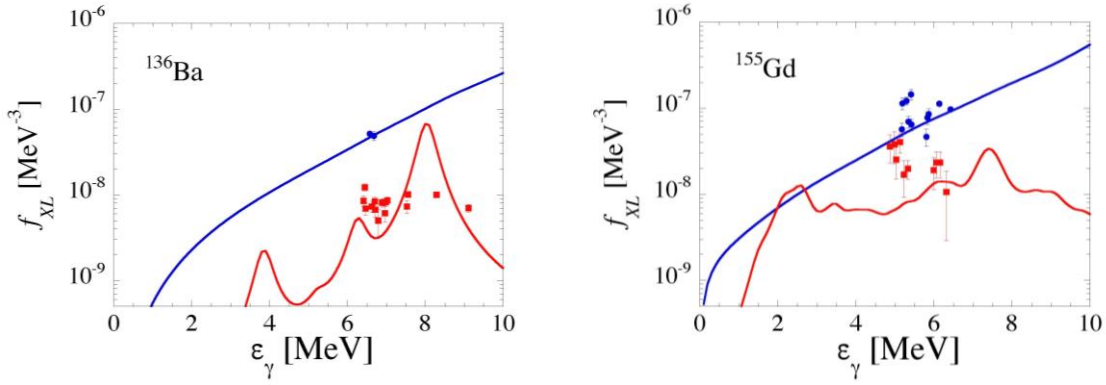

FIG. 8. *A typical distribution of the M1 strength for a spherical (^{136}Ba) and deformed (^{155}Gd) nuclide from QRPA calculations.*

Indeed, for deformed nuclei QRPA calculations give an additional low-energy M1 component corresponding to the scissors mode, which is absent in spherical nuclei, where the spin-flip resonance dominates around 8 MeV [25].

In general, the agreement between D1M+QRPA and ARC data is rather satisfactory, except for a few cases including ^{155}Sm, ^{156,157,159}Gd and ^{165}Dy, where D1M+QRPA underestimate the ARC data. The disagreement may be partly due to the uncertainties in the conversion from I_γ/E^3 into PSF format, which may involve uncertainties in the DRC evaluations. This is supported by the fact that both E1 and M1 strengths are underestimated together. For example, all these nuclides (except for ^{157}Gd) are normalized to the systematics equation, although in this mass region there clearly is a large discrepancy between the DRC measurements and the deduced systematic trend as shown in Fig. 3. In the case of ^{157}Gd, the DRC measurement seems to deviate from the neighbouring data very strongly.

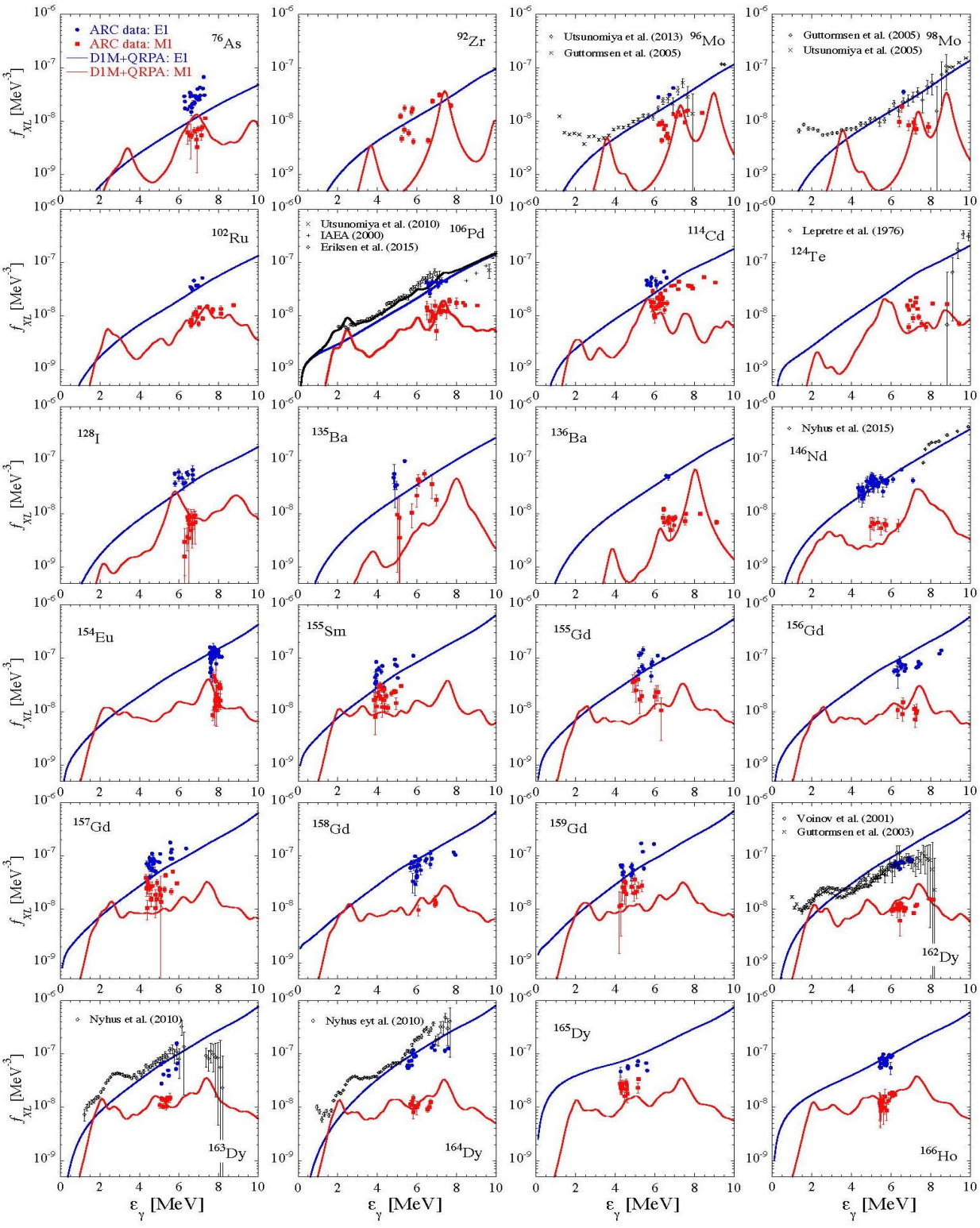

FIG. 9. *Comparison between E1 and M1 strength functions derived from ARC data and D1M+QRPA calculations (Refs. [24,25]) and private communication from S. Goriely. Also shown are the total strength functions extracted from other measurements, in particular (γ,n) cross section or transfer reaction through the Oslo method.*

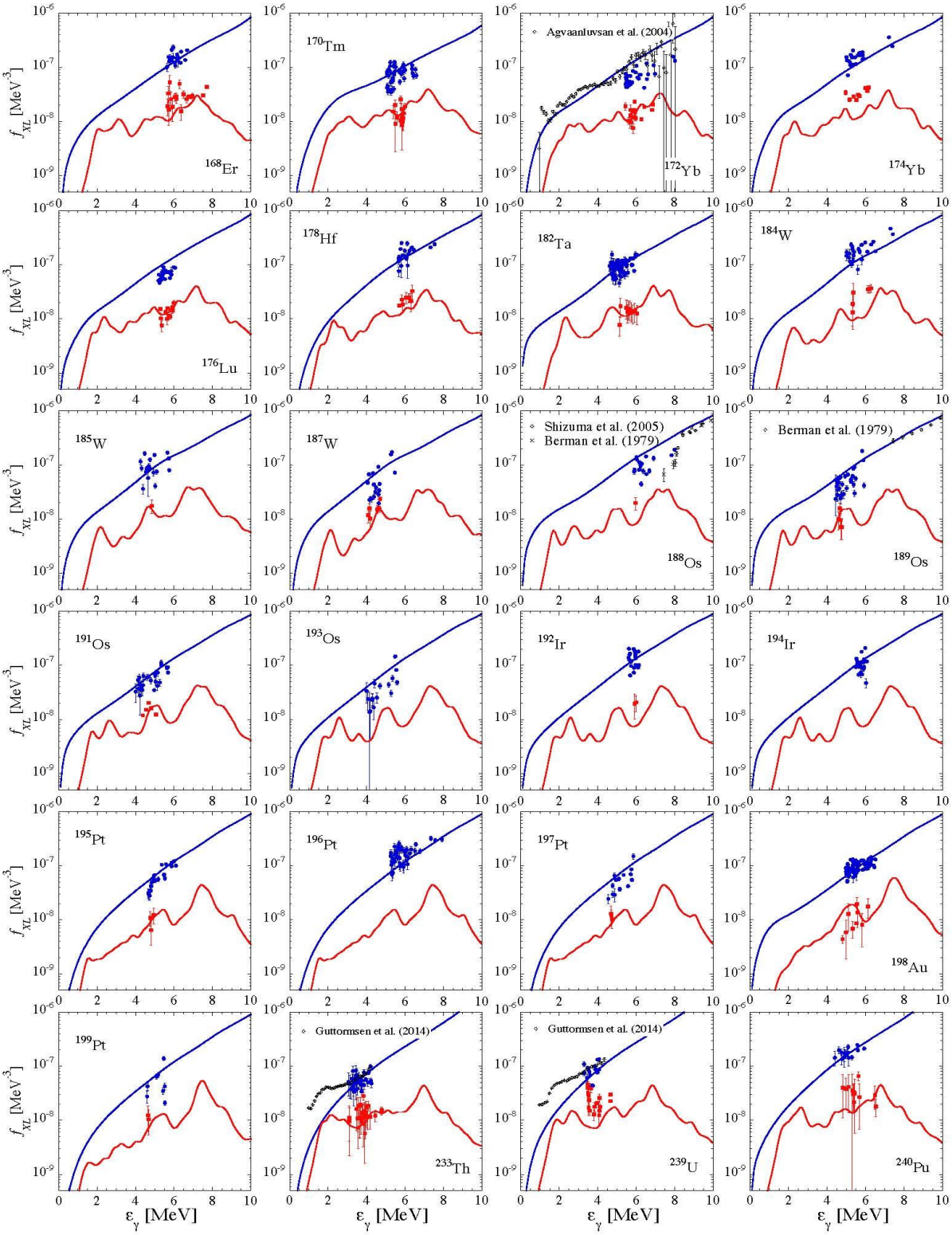

FIG. 10. *Comparison between E1 and M1 strength functions derived from ARC data and D1M+QRPA calculations (Refs. [24,25]) and private communication from S. Goriely. Also shown are the total strength functions extracted from other measurements, in particular (γ,n) cross section or transfer reaction through the Oslo method.*

5. Conclusions

ARC data measured at different filter beam facilities have been re-analysed. They include all measurements made at ANL, INEL and BNL between 1970 and 1990, but have only been partially exploited until now. This is the first time that a comprehensive re-evaluation of all measured data was completed and applied for a systematic comparison with estimated PSF in the mass range $70 < A < 240$. Updated spectroscopic information on the states of interest is used to extract the E1 and M1 transition groups in the PSF. This re-evaluation provides new experimental information on the E1 and M1 strength function around the neutron binding energy and also provides new constraints for existing γ-ray strength models used in statistical reaction codes.

Globally, the revised data agree rather well with the total strength function extracted from photonuclear data or from transfer or inelastic reactions by the so-called Oslo method. The ARC data also show that the recent QRPA calculations based on the D1M Gogny force give rather satisfactory predictions, both for the E1 and M1 strengths. The ratio of the E1 to M1 strength functions is found to remain within the small range of 1.5 and 7.8 but not to follow any clear systematics, as expected from microscopic predictions of different excitation modes for M1 radiation (see Fig. 11). The ARC E1-to-M1 strength ratio represents a new stringent test for the future elaboration of theoretical models for the dipole strength function.

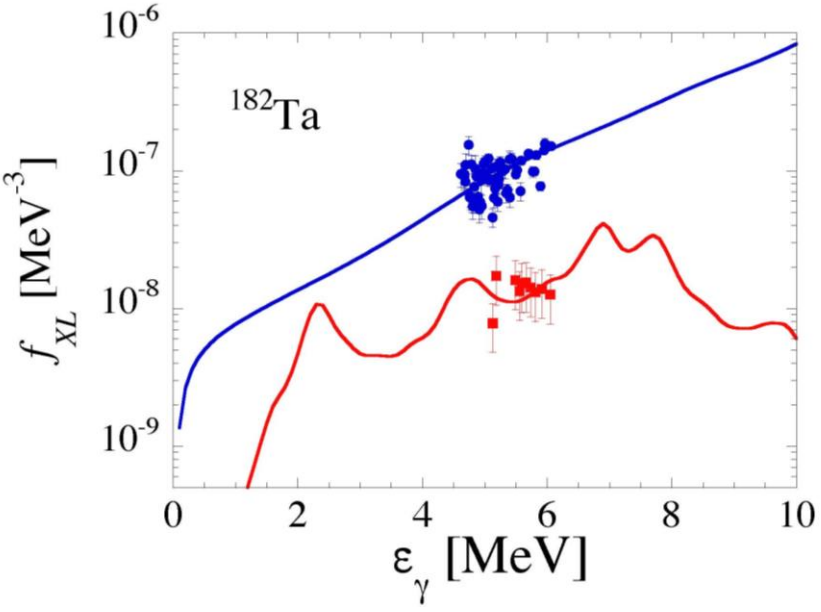

FIG. 11. *Note the complexity of different M1 excitation modes below the spin-flip resonance, strongly influencing the E1/M1 ratio as a function of* E_γ.

The Atlasf(L)[final] will be made available through the IAEA Coordinated Research Project F41032 on Updating the Photonuclear data Library and generating a Reference Database for Photon Strength Functions or from the author on request. The whole data packet consists of three data files, see below:

Data file	Content
AtlasI$_\gamma$/E$_\gamma^3$	Includes data from adopted measurements and reduced by E_γ^3. The assignment to E1, M1 and E2 multipolarity groups is carried out, based on ARC results and J^π assignments.
Atlasf(L)	*AtlasI$_\gamma$/E$_\gamma^3$* data converted in 10^{-8}MeV^{-3} scale by normalization to the DRC information. The correction for single population of $J_f = I_t \pm 3/2$ applied.
Atlasf(L)[final]	*Atlasf(L)* data corrected for the $<E_\gamma>$ dependence of the DRC normalization. Furthermore, the M1 general p-wave corrections were applied. **The final version (August 2017)**

Acknowledgments

The author acknowledges the long and fruitful collaboration with the late R.E. Chrien and also acknowledges the inspiration and continuous support by S. Goriely. F. Becvar who contributed with many fruitful discussions and awarding access to old data. This work was performed within an IAEA Nuclear Data Section Special Service Agreement.

References

[1] L.M. Bollinger and G.E. Thomas, Phys.Rev. **C2** (1970) 1951, and L.M. Bollinger: Proceedings Int Conf. on Photonuclear Reactions and Applications, Pacific Grove, 1973, (Ed.: B.L. Berman), Lawrence Livermore Laboratory report CONF-730301, p. 783.

[2] R.B. Schwartz, *et al.*, Proc. Int. Symp. on Neutron Capture Gamma-ray Spectroscopy and related Topics, Petten (NH) (1974) 346.

[3] G.A. Bartholomew, *et al.*, Adv. Nucl. Phys. **7** (1973) 229.

[4] M.A. Lone, Neutron Gamma Ray Spectroscopy and Related Topics, Plenum, New York, 1979, p. 161.

[5] R. Greenwood and C. Reich, Nucl. Phys. A **223** (1974) 66.

[6] R. Greenwood and R. Chrien, Nucl. Instr. Meth. **138** (1976) 125.

[7] M.L. Stelts, in: Nuclear Cross Section for Technology, Nat. Bur. Of Stds. Sp. Publ. 594, 1980, p. 936. 3.

[8] R.E. Chrien, Neutron-Capture Gamma-Ray Spectroscopy and related Topics, Institute of Physics Conf. Series, No 62, p. 342.

[9] J. Kopecky, "Neutron Gamma Ray Spectroscopy and Related Topics" Knoxville, (Tennessee (1984) 318.

[10] R.E. Chrien, "Fourth Int. Symposium on Neutron Induced Reactions", Smolenice (CZ) (1985) 200.
[11] R.E. Chrien, "5rd Int. School on Neutron Physics", Alushta (USSR) CONF-8610176—2 October 1986 and BNL-38900 report.
[12] A.F. Gamalii, *et al.,* Sov. J. Nucl. Phys **15**, (1972) 1.
[13] A.V. Murzin, *et al.,* Proc. 40th Ann. Conf. Nucl. Structure At. Nuclei, (Leningrad 1990) 86.
[14] H. Ottmar, *et al.*, Proc. Int. Symp. on Neutron Capture Gamma-ray Spectroscopy and related Topics, Petten (NH) (1974) 658.
[15] R. Chrien, J. Kopecky, H. Liou, O. Wasson, J. Garg, and M. Dritsa, Nucl. Phys. A **436** (1985) 205.
[16] J. Kopecky and R. Chrien, Nucl. Phys. A **468** (1987) 285.
[17] J. Kopecky and M. Uhl, Phys. Rev. C **41** (1990) 1941.
[18] J. Kopecky, M. Uhl and R.E. Chrien, Phys. Rev. C **47** (1983) 312.
[19] J. Kopecky, S. Goriely, S. Peru, S. Hilaire, M. Martini, E1 and M1 strength functions from average resonance capture data, Phys. Rev. C **95** (2017) 054317.
[20] R. Capote, *et al.*, Nuclear Data Sheets **110** (2009) 3107.
[21] U. Mayerhofer, *et al.*, Nucl. Phys. A **492** (1989) 1.
[22] J. Kopecky, Present Status of Experimental Gamma-ray Strength Functions Derived from Neutron Capture, IAEA report INDC(NED)-013 (September 2016).
[23] J. Kopecky, ECN-RX-92-011, Tech. Rep. 011, ECN (1992).
[24] M. Martini et al. Phys. Rev. C **94** (2016) 014304.
[25] S. Goriely et al., Phys. Rev. C **94** (2016) 044306.

APPENDIX

TABLE 1. LIST OF RECOVERED ARC MEASUREMENTS WITH NEUTRON FILTERED BEAMS (B, Sc or Fe) SELECTED FOR THE FINAL PSF DATA BASE. (*Selected ARC data for the PSF data base are denoted with red x. "[Ref] BNL/ECN" stands for the data from quoted references processed and included in the BNL/ECN data base.)*

Product nuclide	**B**	**Sc**	**Fe**	**Final *ATLAS f(L)***	**Excluded measurements**
Ti-49		x	x	[1]	Poor averaging
Co-60			x	[2]	24 keV only
Cu-64		x		[3]	Poor averaging
Cu-66		x		[4]	Poor averaging
As-76		x		[5]	
Zr-92		x		[6]	
Mo-96		x		[7] BNL/ECN	
Mo-98		x		[7]	
Ru-102		x		[8]BNL/ECN	
Pd-106	x	x		[9] BNL/ECN	[10][11][12] BNL/ECN
Ag-108		x		[13]	No Iγ data
Cd-114		x		[14] BNL/ECN	
Te-124		x		[15]	
I-128		x		[12]	
Ba-135		x		[16]	
Ba-136		x		[17]	
Ce-136		x	x	[18]	No Iγ data
Nd-146	x	x		[19]	[20]
Sm-155		x		[21] BNL/ECN	
Eu-154		x		[22]	
Gd-155		x		[23]	[24][25]
Gd-156	x	x		[9] BNL/ECN	[26][27]
Gd-157		x		[24]BNL/ECN	[25]
Gd-158	x	x		[9]	[28]
Gd-159		x		[38]	[29]
Gd-161		x		[25]	
Dy-162		x		[30] BNL/ECN	
Dy-163		x		[31]	
Dy-164		x		[30] BNL/ECN	
Dy-165		x		[32]	
Ho-166	x			[9]	
Er-168	x	x		[9] BNL/ECN	

Product nuclide	B	Sc	Fe	Final *ATLAS f(L)*	Excluded measurements
					[33]
Tm-170		x		[34]	
Yb-172		x		[35] [BNL/ECN	
Yb-174		x		[36]	[46]
Lu-176		x		[38] BNL/ECN	
Hf-178		x		[39]	
Ta-182		x		[49]	
W-184	x	x		[41]	[42]
W-185		x		[43]	
W-187		x		[43]	
Os-188		x		[44]	
Os-189		x		[45]	
Os-191		x		[46]	
Os-193		x		[47]	
Ir-192		x		[48]	
Ir-194		x		[49]	
Pt-195		x		[50] BNL/ECN	
Pt-196		x		[51]	
Pt-197		x		[52]	
Pt-199		x		[52]	
Au-198		x		[53]	
Th-233		x		[54] BNL/ECN	
U-236		x		[55]	
U-239	x	x		[56] BNL/ECN	[57] BNL/ECN
Pu-240		x		[58]	

Filtered beams ARC data :

[1] A.F. Gamalii et al., Sov.J.Nucl.Phys. 15(1972) 1 *Ti-49, Mo-96,98*
[2] J. Kopecky et al., Nucl. Phys.A427 (1984) 413 *Co-60*
[3] M.G. Delfini et al., Nucl. Phys. A404 (1983) 225 *Cu-64*
[4] M.G. Delfini et al., Nucl.Phys. A404 (1983) 250 *Cu-66*
[5] F. Hoyler at al., Nucl.Phys. A512 (1990) 189 *As-76*
[6] M.J. Kenny at al., *Proceedings of Neutron Gamma Ray Capture Spectroscopy and related topics, BNL,*(Upton 1978) 676 and BNL- 24698 *Zr-92,93,95*
[7] K. Rimavi and R.E. Chrien, Phys.Rev. C15 (1977) 1271 *Mo-93,95,97,99*
[8] BNL/ECN database (unpublished BNL data) *Mo-96,Ru-102, Pd-106*
[9] L.M. Bollinger and G.E. Thomas, Phys.Rev. C2 (1970) 1951 *Pd-106, Gd-156,158, Ho-166, Er-168*
[10] J. Kopecky and R.E. Chrien, Nucl.Phys. A468 (1987) 285 *Pd-106*
[11] B. Fogelberg et al., Nucl.Phys. A475 (1987) 301 *Pd-106*

[12] C. McCullagh, Univ. Stony Brook Thesis, (1978) *Pd-106, I-128*
[13] T.D. MacMahon et al., J.Phys. G11 (1985) 1231 *Ag-108, Gd-158*
[14] A. Meemeed et al., NP A412 (1984) 113 *Cd-114*
[15] R.F. Casten et al., Phys.Rev. C44 (1991) 523 *Te-124*
[16] R.E. Chrien et al., Phys.Rev. C48 (1973) 109 *Ba-135*
[17] K. Schreckenbach et al., *Capture Gamma-Ray Conf. Proc*., 1981) 200 *Ba-136*
[18] B.K. Koene et al., priv. com. 1981 *Ce-136*
[19] D.L. Bushnell et al., Phys.Rev. C14 (1975) 75 *Nd-146*
[20] S. Raman et al., J.Phys. G9 (1983) L137 Nd-146
[21] K. Schreckenbach et al. Nucl.Phys. A376 (1982) 149 *Sm-155*
[22] M.A. Balodis et al., Nucl.Phys. A572 (1987) 445 *Eu-154*
[23] H.H. Schmidt et al., J.Phys. (London) G12 (1986) 411*Gd-155*
[24] R.C. Greenwood et al., *Proceedings of Neutron Gamma Ray Capture Spectroscopy and related topics*, RCN Petten (September 1974) *Gd-155,157*
[25] R.G. Greenwood and R.E. Chrien, Bull. Am. Phys. Soc. 22 No.8 ED9 (1977) 1032 *Gd-155,157,159,161*
[26] A. Backlin et al., Nucl.Phys.A380(1982) 189 *Gd-156*
[27] J. Kopecky et al., Phys.Rev. C47(1993) 312 *Gd-156*
[28] R.C. Greenwood et al., Nucl.Phys. A304 (1978) 327 *Gd-158*
[29] C. Granja et al., Nucl.Phys. A279 (2003) 679 *Gd-159*
[30] D.D. Warner et al., Phys.Rev. C27(1983) 2292 *Dy-162,164*
[31] H.H. Schmidt, et al., Nucl. Phys. A504 (1989) 1 *Dy-163*
[32] E. Kaerts et al., Nucl.Phys. A514 (1990) 173 *Dy-165*
[33] W. Davidson et al., J.Phys. G7 (1981) 843 *Er-168*
[34] R.W. Hoff et al., Phys. Rev. C (1996) 78 *Tm-170*
[35] R. C. Greenwood et al., Nucl.Phys. A252(1975) 260 *Yb-172*
[36] C. Granja et al., Nucl.Phys. A757(2005) 287 *Yb-174*
[37] R.C. Greenwood et al., Phys.Rev. C23(1981) 153 *Yb-174*
[38] R.W. Hoff et al., Nucl.Phys. A437 (1985) 285 *Lu-176*
[39] A. Hague et al., Nucl.Phys. A455 (1986) 231*Hf-178*
[40] R.G. Helmers et al., Nucl.Phys, A168 (1971) 449 *Ta-182*
[41] R.C. Greenwood et al., Nucl.Phys. A223 (1974) 66 *W-184*
[42] D.L. Buschnell et al., Phys. Rev. C11 (1975) 1401 *W-184*
[43] A.M. Bruce et al., Nucl. Phys. A465 (1987) 221 *W-185,187*
[44] A.V. Murzin, *et al.*, Proc. 40th *Ann. Conf. Nucl. Structure At. Nuclei*, (Leningrad 1990) *86 Os-188*
[45] A.M. Bruce et al., Nucl. Phys. A452 (1992) 1 *Os-189*
[46] R.F. Casten et al., Nucl. Phys. A285 (1977) 235 *Os-191*
[47] D. D. Warner et al., Nucl.Phys. A316 (1979) 13 *Os-193*
[48] J. Kern et al., Nucl. Phys. A534 (1991) 77 *Ir-192*
[49] M. Balodis et al., Nucl. Phys. A641 (1998) 133 *Ir-194*
[50] D.D. Warner et al., Phys.Rev. C26 (1982) 1921 *Pt-195*
[51] J. Cizewski et al., Nucl. Phys. A323 (1979) 349 *Pt-196*
[52] R.F. Casten et al., Phys. Rev. C 27(1983) 1310 *Pt-197, 199*
[53] U. Mayerhofer et al., Nucl.Phys. A492(1989) 1 *Au-198*
[54] P. Jeuch et al., Nucl.Phys. A317 (1979) 363 *Th-233*
[55] H. Ottmar et al., *Proc, Int. Symposium on Neutron Capture Gamma-rays Spectroscopy and related Topics*, Petten (NH) (1974) 658 *U-236*
[56] L.M. Bollinger and G.E. Thomas, Phys.Rev. C6(1972) 1322 *U-239*

[57] R.E. Chrien and J. Kopecky, Nucl. Phys. A414 (1984) 281 *U-239*
[58] R.E. Chrien et al., Nucl.Phys. A436 (1985) 205 *Pu-240*

TABLE 2. AN EXAMPLE OF ***ATLASIGE3*** **FILE** FOR AS-76 DATA

As -76 2 keV data from BNL

Ig/Eg**5 extracted from F. Hoyler et al., Nucl.Phys. A 512 (1990) 189 converted in Ig/Eg**3

D - unresolved doublet

E(gamma)	E1	M1	E2	dE1	dM1	dE2	Ex	Jπ
7329		65.9			2.69		0	2-
7285	142.76			2.65			44	1+
7242	312.58			1.05			87	1+
7208	188.6			2.08			121	1+
7164		43.82			4.11		165	3-
7126		31.31			4.57		203	(0,1)+
7119			16.22			7.6	210	4-
7064	140.22			2			264	1+,2+
7049	198.26			1.49			280	1+,2+
7029	117.59			7.91			300	(2,3)
7021	133.09			1.97			307	2+
7002			11.28			9.81	329	3-4-
6977	116.83			4.87			352	3-
6965		41.21		0	3.4		363	1-,2-
6927	186.18			1.44			402	1+,2+
6897		18.76			9.51		436	1-2-3-
6882	123.14			2.37			447	1+,2+
6873		26.37			6.61		456	2-3-
6858							471/D	2-
6830	135.75			2.8			500	1+,2+
6824	134.11			11.18			505	2+3+
6811							518/D	1+,2+
6785	101.15			8.51			544	0+3+
6779		38					550	2-3-
6719	102.03			9.93			609	2+3+
6700	138.26			2.24			628	2-3-
6692							637/D	1+,2+
6660	96.25			4.44			669	1+,2+
6642	83.38			2.21			687	1,2,3,4
6627		31.22			3.51		703	1,2,3,4
6613	69.1			9.62			715	1+2+3+
6588		30.9			14.76		742	≤3
6584	154.32			3.47			744	1+,2+
6573	134.8			6.91			756	0+3+

6555	88.08		3.01		774	1+2+3+
6544					787/D	≤3
6536	161		2.5		794	(1+2+3+)
6528		31.32		5.11	801	3+1-2-
6466					861/D	(1+2+3+)
6433		35.59		10.76	894	3+1-2-
6420	78		3		909	1+,2+
6407					926/D	
6390					940/D	(1-3)
6344			1.61		985	(1-3)+
6308					1021	
6301	80.2		5.16		1028	1+,2+
6296	108.22		3.96		1032	1+,2+
6266	136.24		1.57		1063	1+,2+

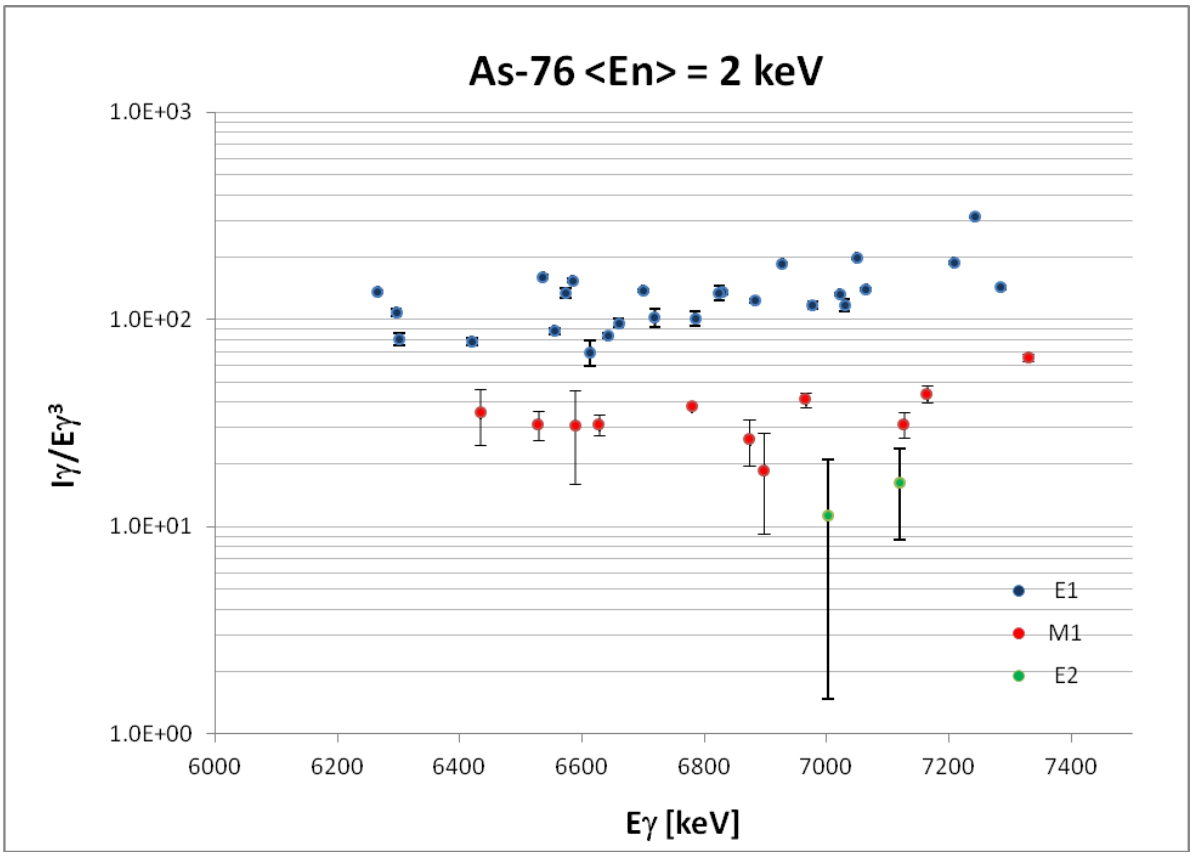

TABLE 3. AN EXAMPLE OF ***ATLAS_F(L)*** **FILE** FOR AS-76 DATA

As -76 2 keV data from BNL

Ig/Eg**5 extracted from F. Hoyler et al., Nucl.Phys. A 512 (1990) 189 converted in Ig/Eg**3 in arbitrary units
The Q(JiJf) correction: the simplified Q(JiJf) = 2 has been applied
Normalization of 9 E1 (<Eg> = 6.67 MeV) transitions to <f(E1)> = 2.35E-08 from <f(E1)> systematic equation

E(gamma)	E1	M1	E2	dE1	dM1	dE2	Ex	Jpi	Q(JiJf)
7329		1.43			0.06		0	2-	
7285	3.09			0.06			44	1+	
7242	6.77			0.02			87	1+	
7208	4.09			0.05			121	1+	
7164		0.95			0.09		165	3-	
7126		0.67			0.11		203	(0,1)+	
7119			0.35			0.18	210	4-	
7064	3.04			0.05			264	1+,2+	
7049	4.29			0.03			280	1+,2+	
7029	2.55			0.18			300	(2,3)	2
7021	2.88			0.05			307	2+	
7002			0.25			0.23	329	3-4-	
6977	2.53			0.11			352	3-	
6965		0.89			0.08		363	1-,2-	
6927	4.03			0.03			402	1+,2+	
6897		0.41			0.22		436	1-2-3-	
6882	2.67			0.05			447	1+,2+	
6873		0.57			0.15		456	2-3-	
6858							471/D	2-	
6830	2.94			0.06			500	1+,2+	
6824	2.91			0.26			505	2+3+	2
6811							518/D	1+,2+	
6785	2.19			0.2			544	0+3+	2
6779		0.83			0.09		550	2-3-	
6719	2.21			0.23			609	2+3+	2
6700	2.99			0.05			628	2-3-	
6692							637/D	1+,2+	
6660	2.08			0.1			669	1+,2+	
6642	1.81			0.05			687	1,2,3,4	
6627		0.67			0.08		703	1,2,3,4	
6613	1.50			0.22			715	1+2+3+	
6588		0.67			0.34		742	<3	
6584	3.34			0.08			744	1+,2+	
6573	2.92			0.16			756	0+3+	2
6555	1.91			0.07			774	1+2+3+	2
6544							787/D	<3	

6536	3.47		0.06			794	(1+2+3+)
6528		0.67		0.12		801	3+1-2-
6466						861/D	(1+2+3+)
6433		0.77		0.25		894	3+1-2-
6420	1.68		0.07			909	1+,2+
6407						926/D	
6390						940/D	(1-3)
6344			0.04			985	(1-3)+
6308						1021	
6301	1.74		0.12			1028	1+,2+
6296	2.35		0.09			1032	1+,2+
6266	2.95		0.04			1063	1+,2+

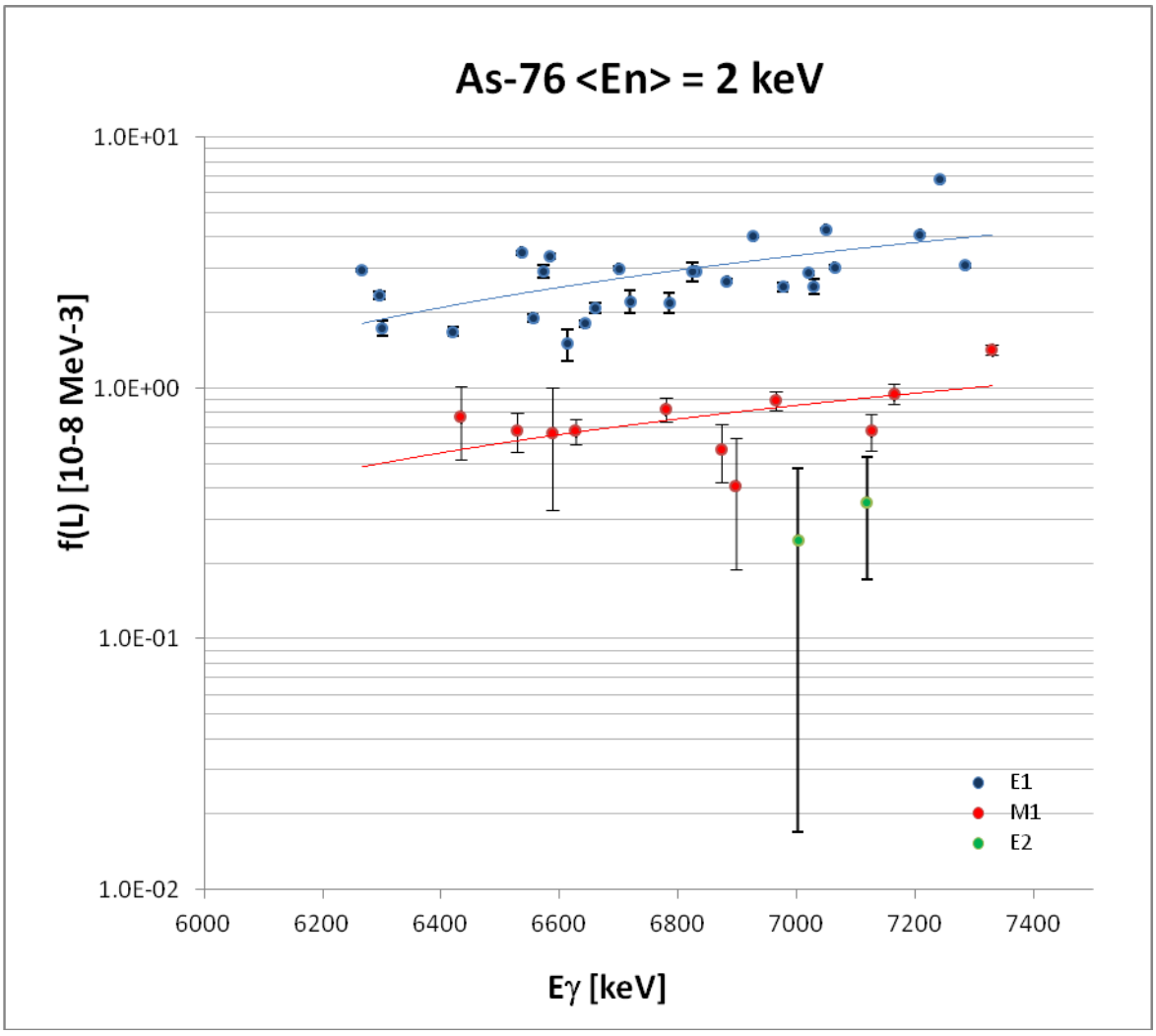

TABLE 4. AN EXAMPLE OF ***ATLAS_F(L)FINAL*** **FILE** FOR As-76 DATA

As -76 2 keV data from BNL

Ig/Eg**5 extracted from F. Hoyler et al., Nucl.Phys. A 512 (1990)189 converted in Ig/Eg**3 in arbitrary units
The Q(JiJf) correction: the simplified Q(JiJf) = 2 has been applied
Normalization of 9 E1 (<Eg> = 6.67 MeV) transitions to <f(E1)> = 2.35E-08 from DRC <f(E1)> systematic equation [INDC(NED)-013]
M1 corrected for 0.19 E1 p-waves contribution from empirical estimate
Uncertainty of PSF: The experimental statistical error is quoted
Porter-Thomas dispersion estimate: 1+dPT=√2/υ=1.44

E(gamma)	E1	M1	E2	dE1	dM1	dE2	Ex	Jpi	Q(JiJf)
7329		1.15			0.06		0	2-	
7285	3.09			0.06			44	1+	
7242	6.77			0.02			87	1+	
7208	4.09			0.05			121	1+	
7164		0.77			0.09		165	3-	
7126		0.55			0.11		203	(0,1)+	
7119			0.35			0.18	210	4-	
7064	3.04			0.05			264	1+,2+	
7049	4.29			0.03			280	1+,2+	
7029	2.55			0.18			300	(2,3)	2
7021	2.88			0.05			307	2+	
7002			0.25			0.23	329	3-4-	
6977	2.53			0.11			352	3-	
6965		0.72			0.08		363	1-,2-	
6927	4.03			0.03			402	1+,2+	
6897		0.33			0.22		436	1-2-3-	
6882	2.67			0.05			447	1+,2+	
6873		0.46			0.15		456	2-3-	
6858							471/D	2-	
6830	2.94			0.06			500	1+,2+	
6824	2.91			0.26			505	2+3+	2
6811							518/D	1+,2+	
6785	2.19			0.2			544	0+3+	2
6779		0.67			0.09		550	2-3-	
6719	2.21			0.23			609	2+3+	2
6700	2.99			0.05			628	2-3-	
6692							637/D	1+,2+	
6660	2.08			0.1			669	1+,2+	
6642	1.81			0.05			687	1,2,3,4	
6627		0.55			0.08		703	1,2,3,4	
6613	1.50			0.22			715	1+2+3+	
6588		0.54			0.34		742	<3	
6584	3.34			0.08			744	1+,2+	

6573	2.92		0.16		756	0+3+	2
6555	1.91		0.07		774	1+2+3+	2
6544					787/D	<3	
6536	3.47		0.06		794	(1+2+3+)	
6528		0.55		0.12	801	3+1-2-	
6466					861/D	(1+2+3+)	
6433		0.62		0.25	894	3+1-2-	
6420	1.68		0.07		909	1+,2+	
6407					926/D		
6390					940/D	(1-3)	
6344			0.04		985	(1-3)+	
6308					1021		
6301	1.74		0.12		1028	1+,2+	
6296	2.35		0.09		1032	1+,2+	
6266	2.95		0.04		1063	1+,2+	

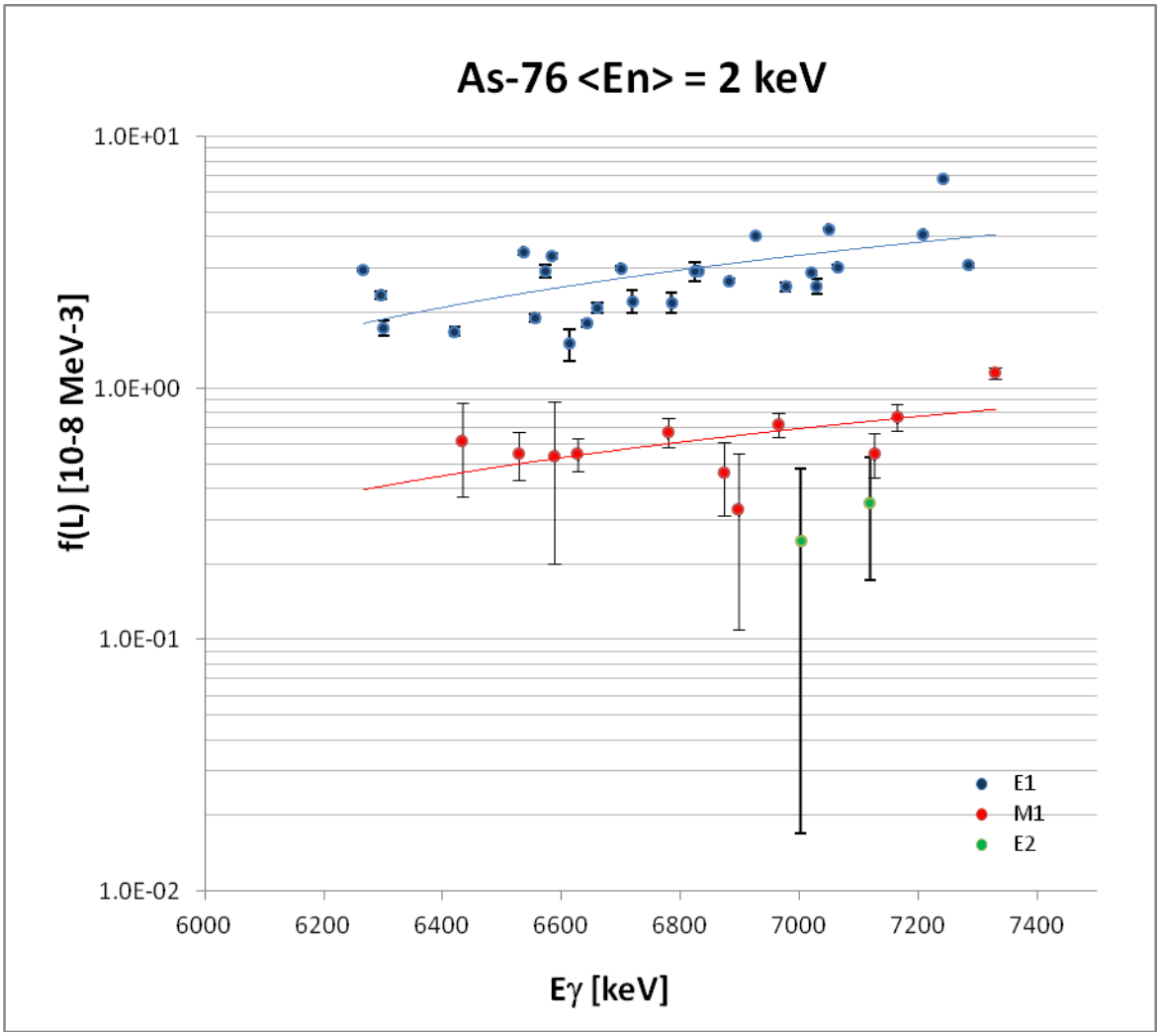

Nuclear Data Section
International Atomic Energy Agency
Vienna International Centre, P.O. Box 100
A-1400 Vienna, Austria

E-mail: nds.contact-point@iaea.org
Fax: (43-1) 26007
Telephone: (43-1) 2600 21725
Web: http://www-nds.iaea.org